

Fig.64 Histopathological examination of liver after i.v. injection of PEG-Ad-TNF α .

Meth-A tumor-bearing BALB/c mice were intravenously injected with Ad-Luc, Ad-TNF α , or PEG-Ad-TNF α (89% modification ratio) at 10^{10} VP/mouse. After 48 h, livers were harvested, placed in neutral 10% formalin, and embedded in paraffin. Sections (5- μ m) were prepared for hematoxylin and eosin staining and histopathological examination. Original magnification is $\times 300$.

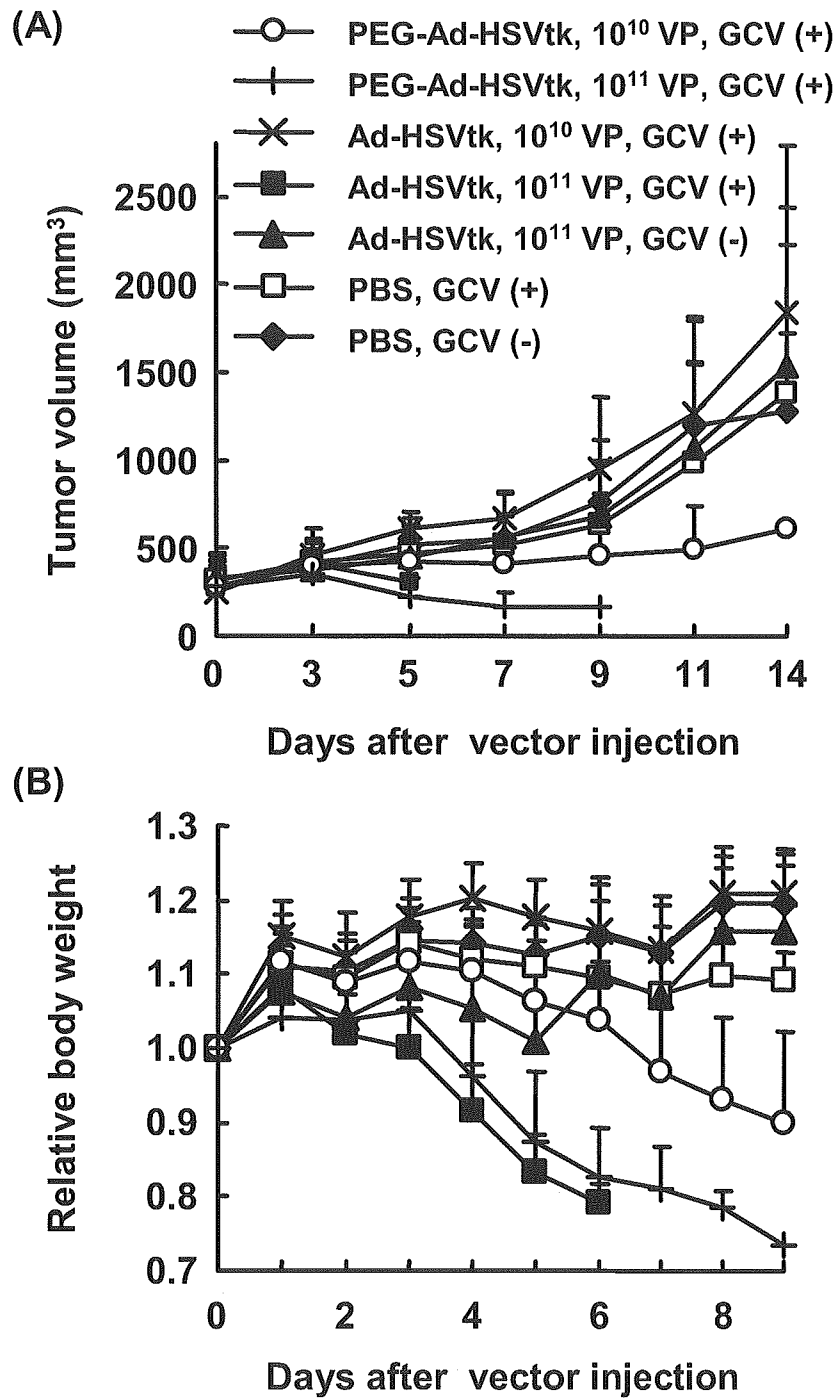


Fig.65 Tumor growth (A) and body weight change (B) in Meth-A tumor-bearing mice treated with HSVtk/GCV system.

Meth-A tumor-bearing BALB/c mice were intravenously injected with Ad-Luc, Ad-HSVtk, or PEG-Ad-HSVtk (90% modification ratio) at 10¹⁰ or 10¹¹ VP/mouse. These mice were treated once daily with intraperitoneal injection of GCV (50 mg/kg/day) for 10 days. The tumor volume (A) and body weight (B) were monitored. Each point represents the mean \pm SD of results from six mice.

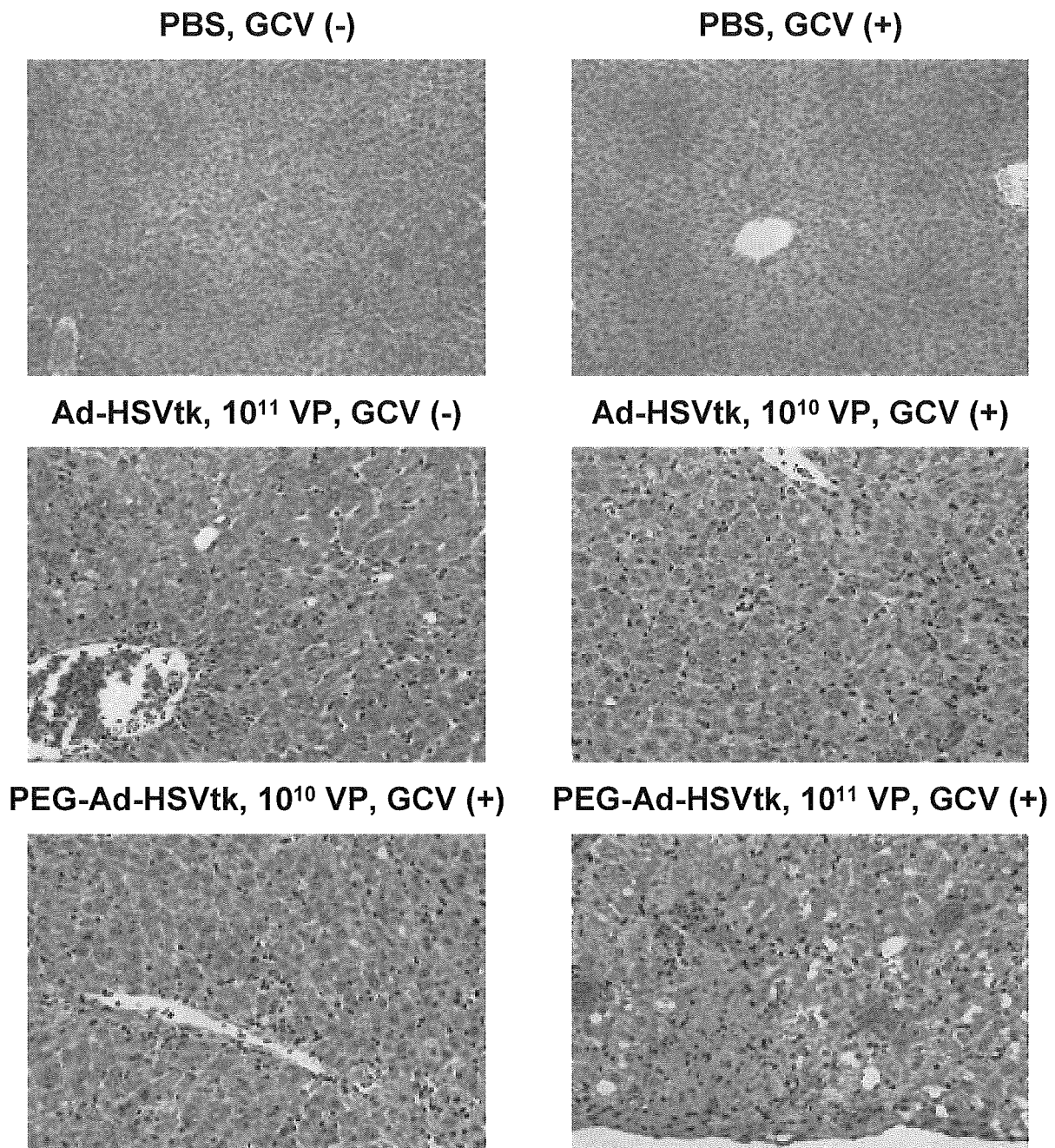


Fig.66 Histopathological examination of liver after HSVtk/GCV treatment.

Meth-A tumor-bearing BALB/c mice were intravenously injected with Ad-HSVtk or PEG-Ad-HSVtk (90% modification ratio) at 10^{10} or 10^{11} VP/mouse. These mice were treated once daily with intraperitoneal injection of GCV (50 mg/kg/day). On day 7 after vector injection, livers were harvested, placed in neutral 10% formalin, and embedded in paraffin. Sections (5- μ m) were prepared for hematoxylin and eosin staining and histopathological examination. Original magnification is $\times 300$.

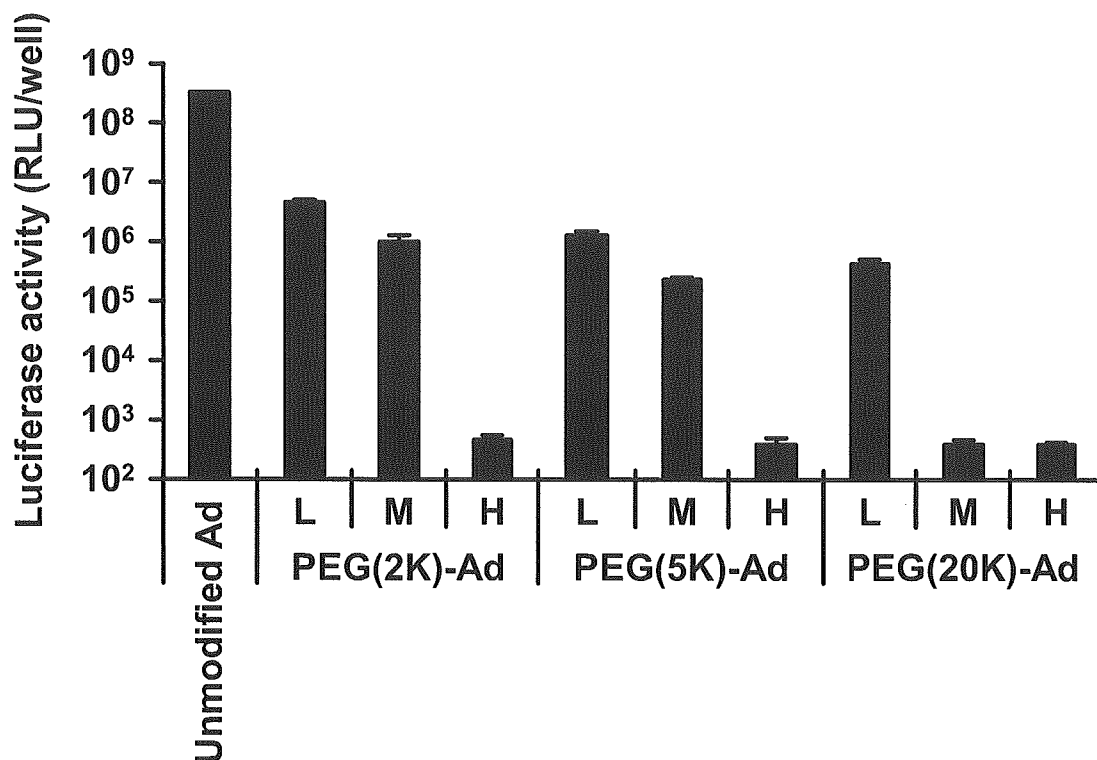


Fig.67 Transduction efficiency of PEG-Ads modified with various PEG.

A549 cells were transduced with unmodified Ad-Luc, PEG(2K)-Ad-Luc, PEG(5K)-Ad-Luc, or PEG(20K)-Ad-Luc at 10000 VP/cell. The modification ratio of PEG-Ad are indicated as follows: L, 30-40%; M, 50-60%; H, 80-90%. After 24 h-cultivation, luciferase activity was measured. Data represents the mean ± SD of results from triplicate culture.

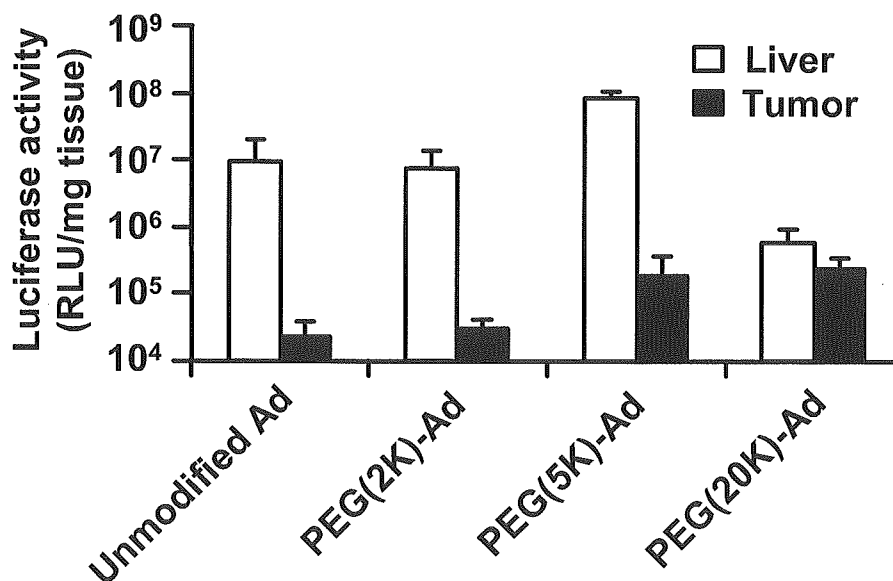


Fig.68 *In vivo* gene expression of PEG-Ads modified with various PEG after i.v. administration into Meth-A tumor-bearing mice.

Meth-A tumor-bearing BALB/c mice were intravenously injected with unmodified Ad-Luc, PEG(2K)-Ad-Luc, PEG(5K)-Ad-Luc, or PEG(20K)-Ad-Luc at 10¹⁰ VP/mouse. Modification ratio of each PEG-Ad was 30-40%. Two days later, liver and tumor were harvested and homogenized with buffer. Luciferase activity was measured using the kit according to the manufacture's instructions. Data represent the mean ± SD or results from five mice.

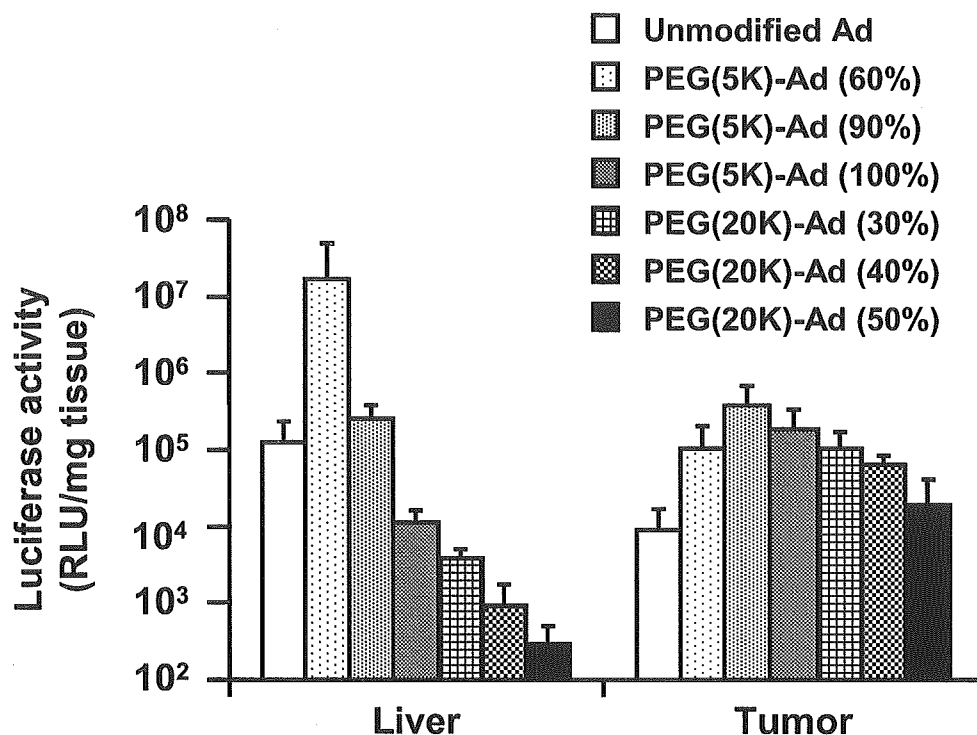


Fig.69 Gene expression pattern in Meth-A tumor-bearing mice injected i.v. with various PEG-Ads. Meth-A tumor-bearing mice were i.v. injected with unmodified or various PEGylated Ad-Luc at 10^{10} VP. Two days later, liver and tumor were harvested and homogenized with buffer. Luciferase activity was then measured using the kit according to the manufacture's instructions. Data represent the mean \pm SE of results from five mice.

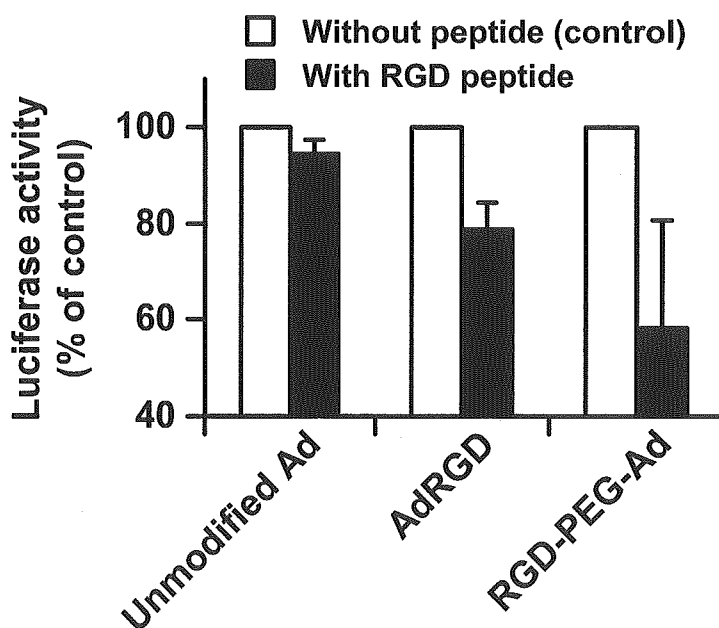


Fig.70 Inhibitory effect of RGD peptide on gene transduction with RGD-PEG-Ad. B16BL6 cells were transduced with unmodified Ad-Luc, AdRGD-Luc, or RGD-PEG-Ad-Luc at 3000 VP/cell in the presence or absence of RGD peptide (200 μ g/ml). Twenty-four hours later, luciferase activity was measured using the kit according to the manufacture's instructions. Data represent the mean \pm SE of results from three independent cultures.

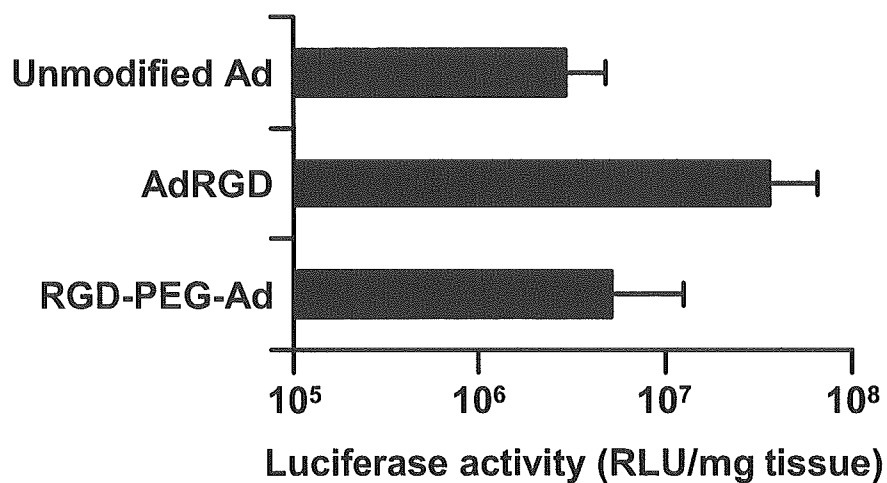


Fig.71 Gene expression in liver of mice injected i.v. with RGD-PEG-Ad.

BALB/c mice were intravenously injected with unmodified Ad-Luc, AdRGD-Luc, or RGD-PEG-Ad-Luc at 1.5×10^{10} VP/mouse. Two days later, livers were harvested and homogenized with buffer. Luciferase activity was then measured using the kit according to the manufacture's instructions. Data represent the mean \pm SE of results from four mice.

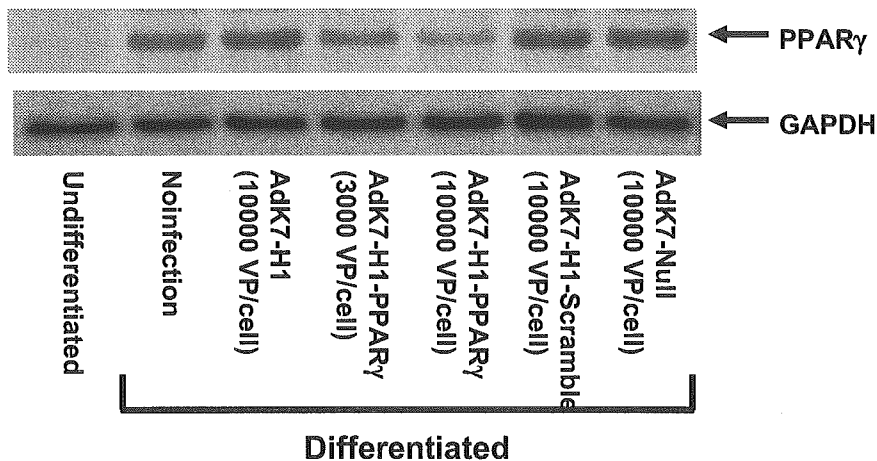


Fig. 72 Suppression of PPAR γ expression in 3T3-L1 cells transduced with AdK7-H1-PPAR γ .

3T3-L1 preadipocytes were transduced with each Ad vector for 1.5 h. On the following day, the cells reached confluence. From three days after Ad treatment, the cells were cultured with differentiation medium containing pioglitazone, insulin, dexamethasone and 3-isobutyl-1-methylxanthine for 4 days. Proteins were then extracted from the cells, and the levels of PPAR γ expression were examined by western blotting. The GAPDH bands served as an internal control for equal total protein loading.

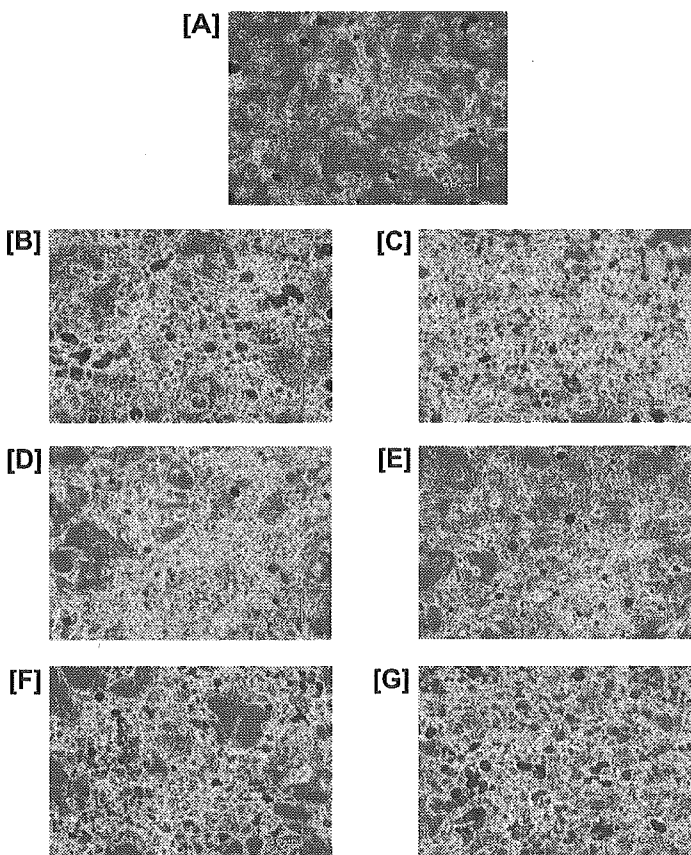


Fig. 73 Suppression of preadipocyte-to-adipocyte differentiation by transduction with AdK7-H1-PPAR γ . 3T3-L1 preadipocytes were transduced with each Ad vector for 1.5 h. On the following day, the cells reached confluence. From three days after Ad treatment, the cells were cultured with differentiation medium containing pioglitazone, insulin, dexamethasone and 3-isobutyl-1-methylxanthine for 9 days. Then, the intracellular lipid accumulation, which was used as the marker of preadipocyte-to-adipocyte differentiation, was determined by Oil red O staining. A, 3T3-L1 preadipocytes (3T3-L1 cells cultured with normal medium); B, 3T3-L1 adipocytes (3T3-L1 cells cultured with differentiation medium without Ad treatment); C, 3T3-L1 cells cultured with differentiation medium with AdK7-H1 (10000 VP/cell) treatment; D, 3T3-L1 cells cultured with differentiation medium with AdK7-H1-PPAR γ (3000 VP/cell) treatment; E, 3T3-L1 cells cultured with differentiation medium with AdK7-H1-PPAR γ (10000 VP/cell) treatment; F, 3T3-L1 cells cultured with differentiation medium with AdK7-H1-Scramble (10000 VP/cell) treatment; G, 3T3-L1 cells cultured with differentiation medium with AdK7-Null (10000 VP/cell) treatment.

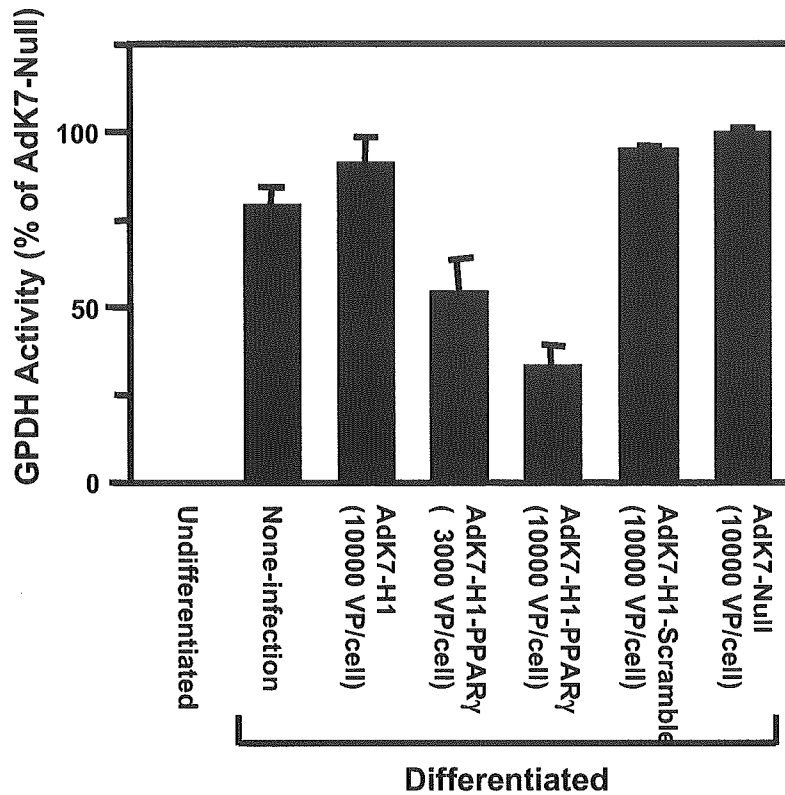
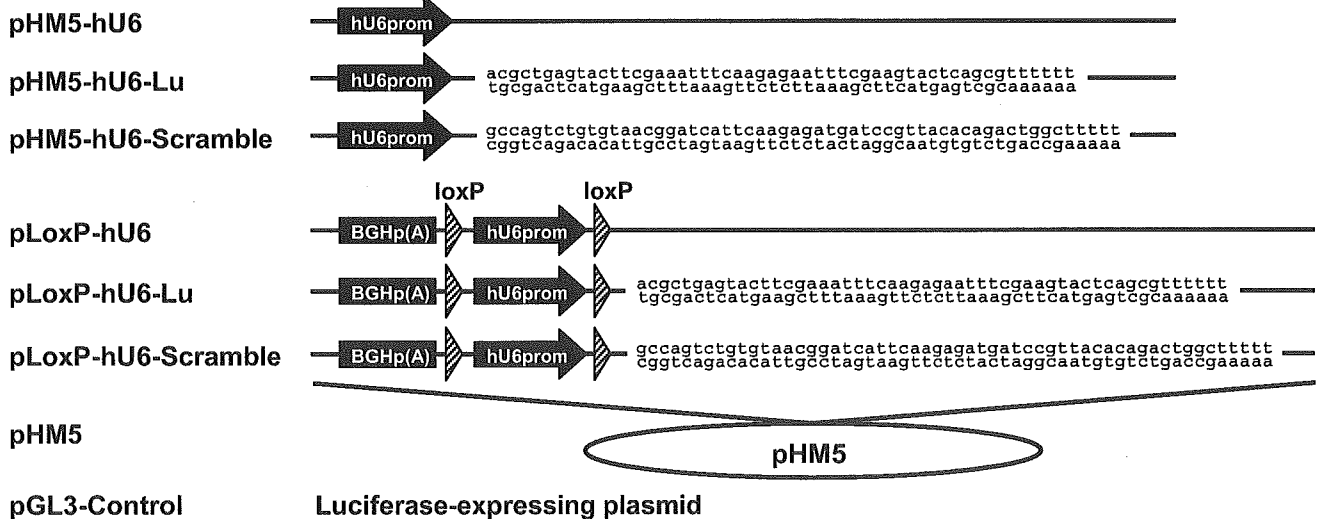


Fig. 74 Suppression of the fatty synthesis on 3T3-L1 cells transduced with AdK7-H1-PPAR γ . 3T3-L1 preadipocytes were transduced with each Ad vector for 1.5 h. On the following day, the cells reached confluence. From three days after Ad treatment, the cells were cultured with differentiation medium containing pioglitazone, insulin, dexamethasone and 3-isobutyl-1-methylxanthine for 9 days. The fatty synthesis was determined by the measurement of GPDH activity in 3T3-L1 cells. Data were expressed as percentage of the GPDH activity of 3T3-L1 cells cultured with differentiation medium with AdK7-Null (10000 VP/cell) treatment.

<Plasmid vectors>



<Adenovirus vectors>

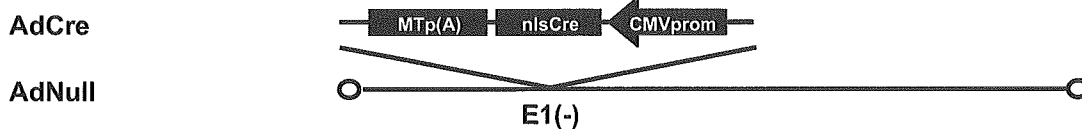


Fig. 75 The structure of plasmid vectors and Ad vectors used in the present study.

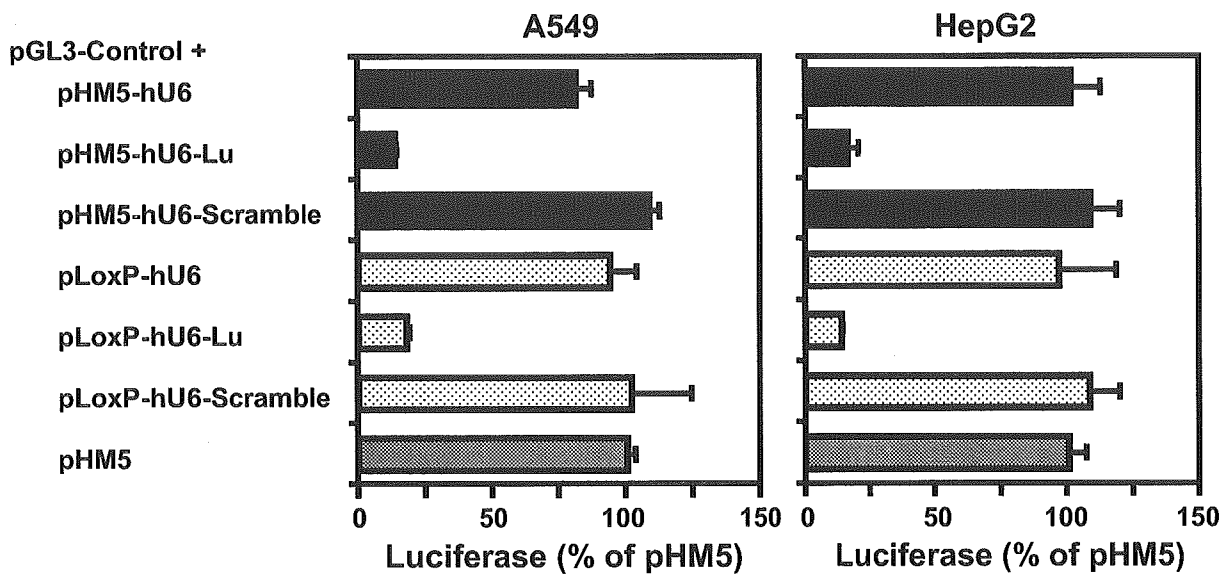


Fig. 76 The effects of insertion of loxP in the plasmid vector expressed siRNA on the suppression of the expression of luciferase.

A549 and HepG2 cells were transfected with each plasmid vector for 2.5 hr, and then cultured for 2 days. The luciferase activity was measured in Materials and Methods.

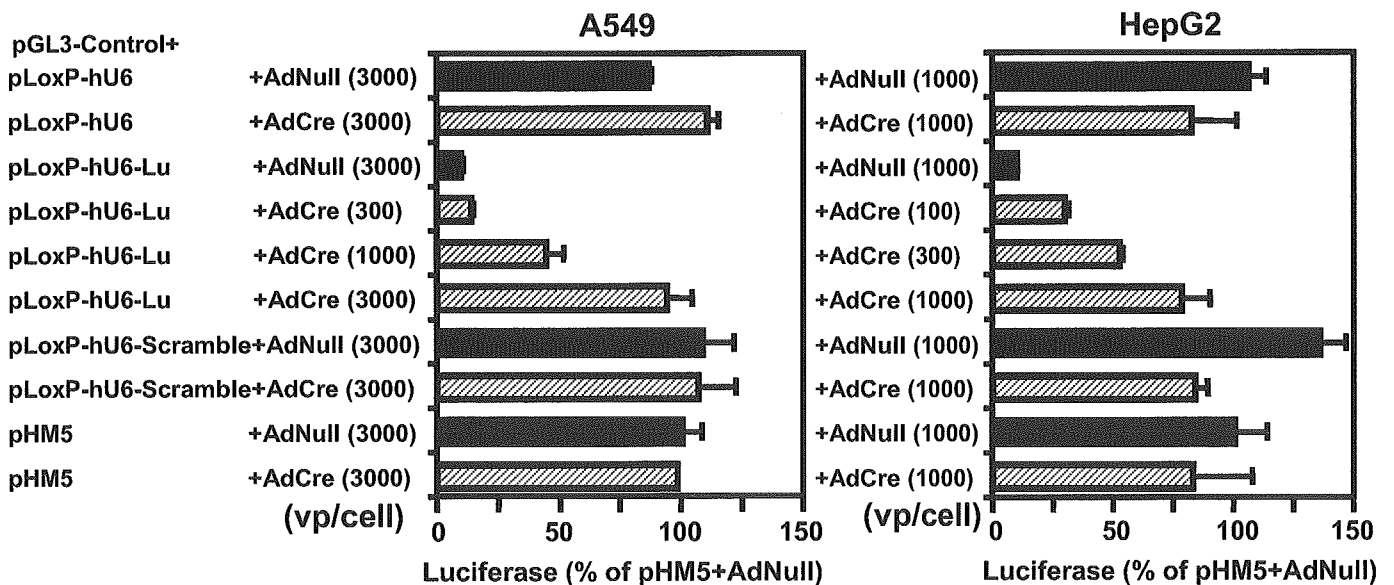


Fig.77 AdCre vector dose-dependent release of the suppressed expression of luciferase by the transfection of pLoxP-hU6-Lu.

A549 and HepG2 cells were infected with AdCre vector for 1.5 hr. The next day, cells were transfected with each plasmid vector for 2.5 hr, and then cultured for 2 days. The luciferase activity was measured in Materials and Methods.

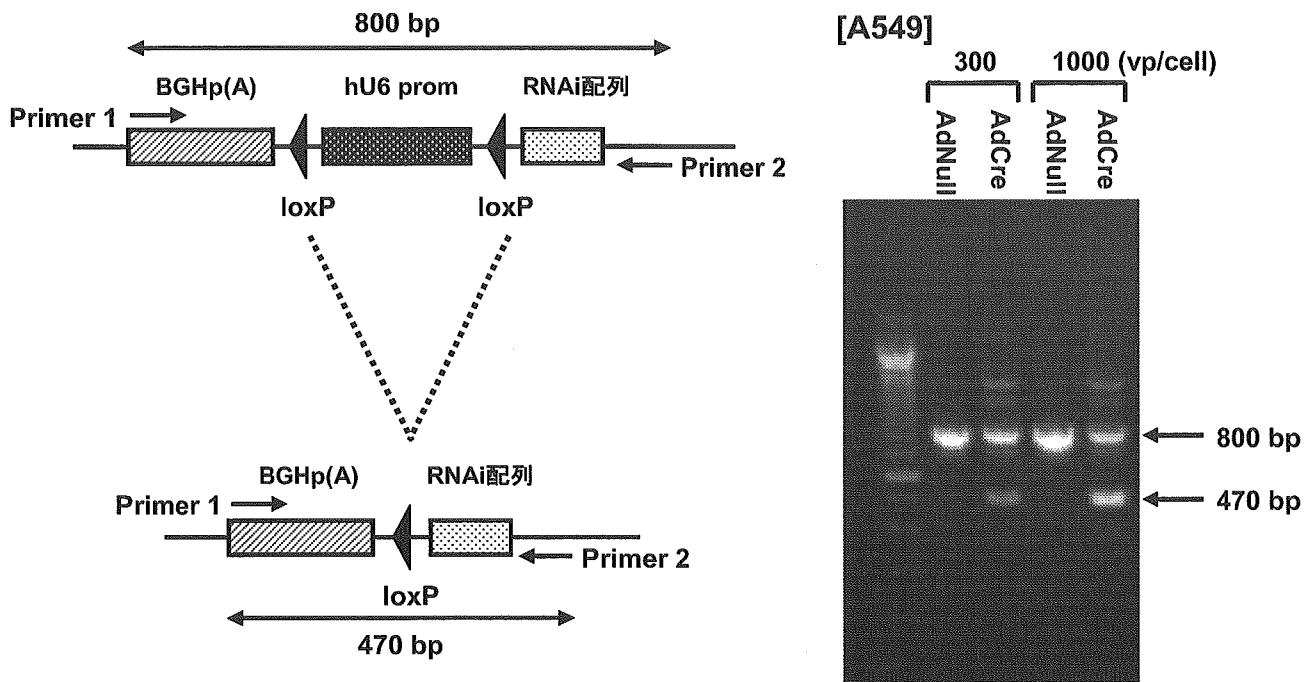


Fig. 78 The removes of hU6 promoter from pLoxP-hU6-Lu treated with AdCre. A549 and HepG2 cells were infected with AdCre vector for 1.5 hr. The next day, cells were transfected with each plasmid vector for 2.5 hr, and then cultured for 2 days. The nuclear DNA was prepared in Materials and Methods.

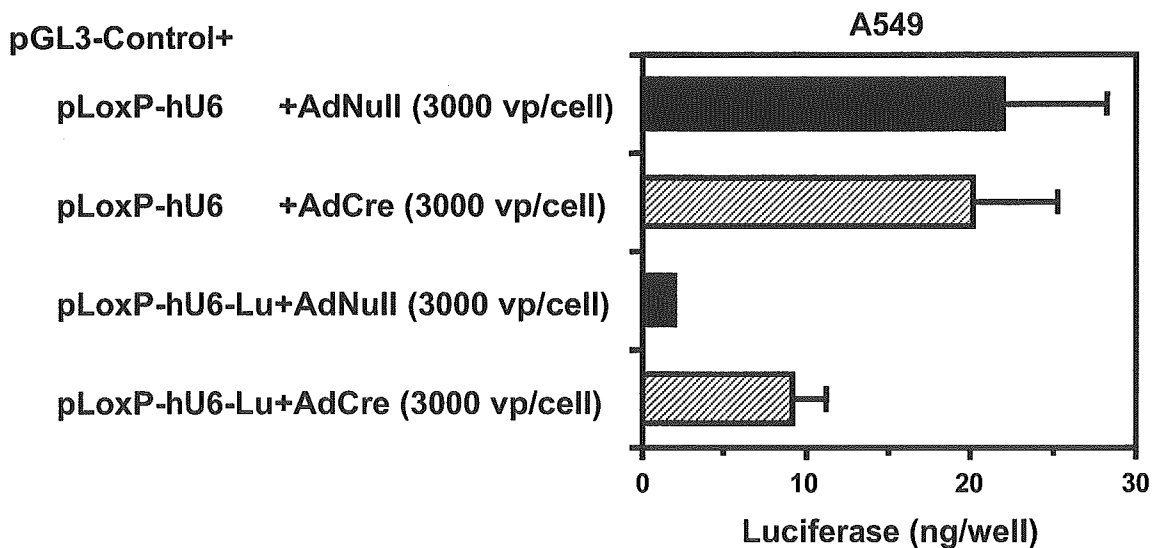


Fig.79 The recovery by the infected AdCre of the suppressed expression of luciferase by the transfection of pLoxP-hU6-Lu.

A549 and HepG2 cells were transfected with each plasmid vector for 2.5 hr. The next day, cells were infected with AdCre vector for 1.5 hr, and then cultured for 4 days. The luciferase activity was measured in Materials and Methods.

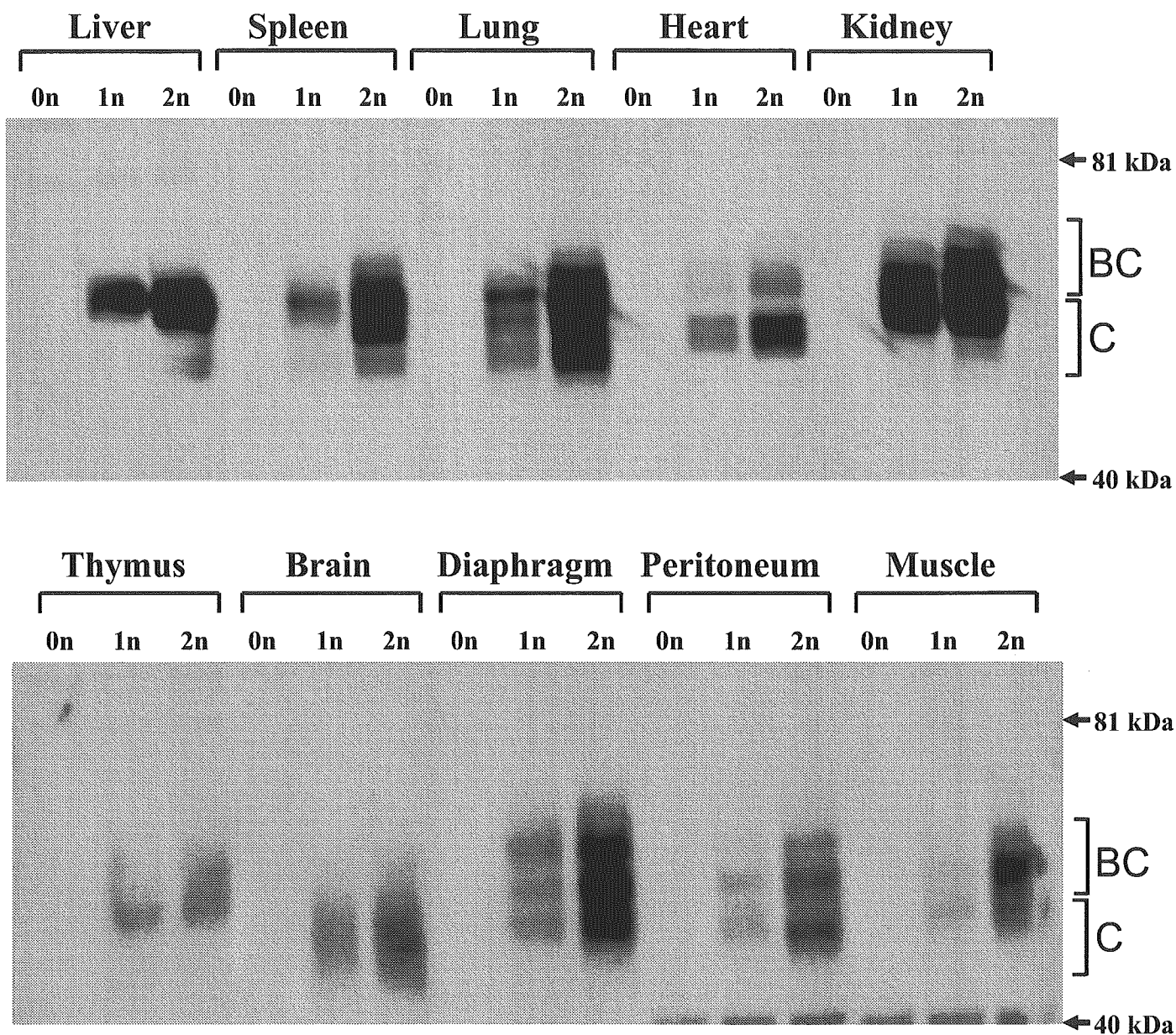


Fig. 80 Human CD46 expression in organs harvested from CD46TG mice.

The protein samples prepared from wild-type mice (0n), hemizygous CD46TG mice (1n), and homozygous CD46TG mice (2n) were separated by sodium dodecyl sulfate-polyacrylamide gel electrophoresis, transferred to a nylon membrane, and reacted against a polyclonal rabbit anti-CD46 serum. The molecular masses of marker proteins (kDa) and approximate positions of the two major isoforms of the CD46 proteins (BC and C isoforms) are indicated on the right.

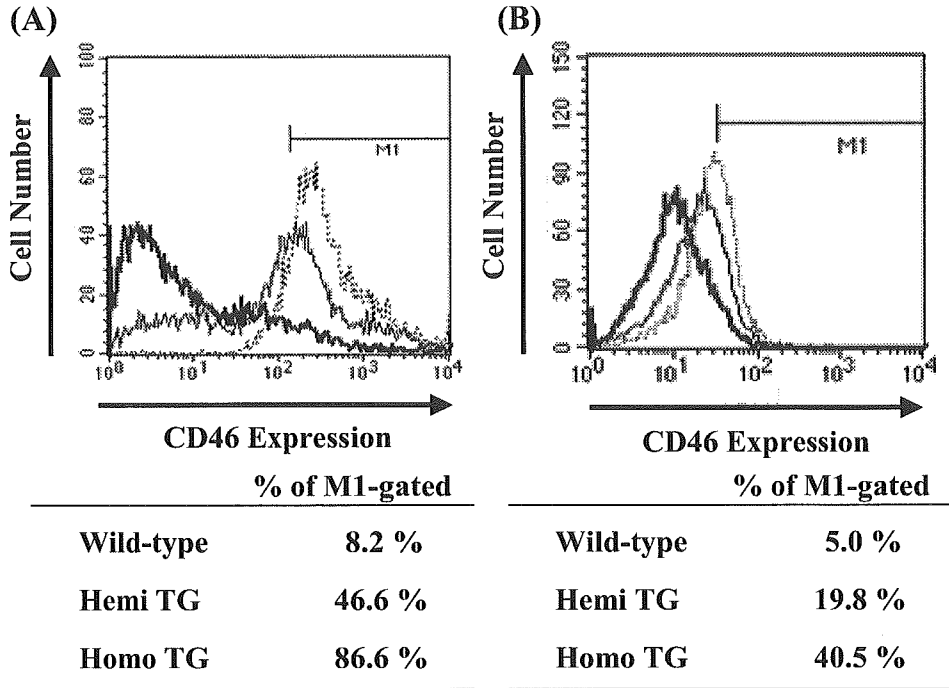


Fig. 81 CD46 expression in (A) mBM-DC and (B) peritoneal macrophages from wild-type mice and CD46TG mice. Thick lines, thin lines, and dotted lines represent cells from wild-type mice (C57B16), and hemizygous (Hemi TG), and homozygous (Homo TG) CD46TG mice, respectively. mBM-DC and peritoneal macrophages were incubated with fluorescein isothiocyanate (FITC)-conjugated anti-human CD46 antibody after incubation with anti-FcγRII/III monoclonal antibody to block nonspecific binding of the anti-human CD46 antibody. After being washed thoroughly, 10⁴ stained cells were analyzed using flow cytometry.

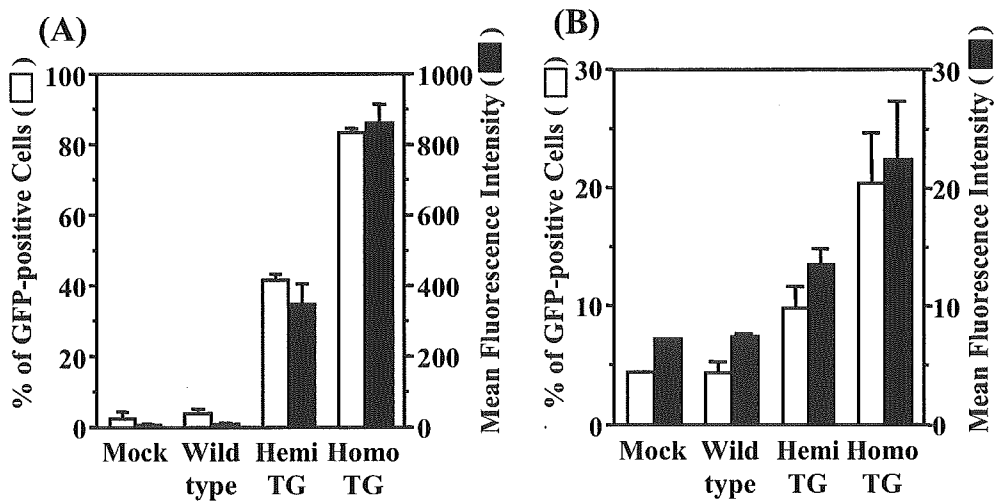


Fig. 82 Ad35 vector-mediated GFP expression in (A) mBM-DC and (B) peritoneal macrophages prepared from wild-type mice and CD46TG mice. Open bars represent percentages of cells positive for GFP, and closed bars indicate mean fluorescence intensity. mBM-DC and peritoneal macrophages prepared from wild-type mice and hemizygous (Hemi TG) and homozygous (Homo TG) CD46TG mice were transduced with Ad35 vectors at 3000 VP/cell for 1.5 h. After a total of 48 h of incubation, GFP expression in cells was evaluated by flow cytometric analysis. The results are represented as mean \pm S.D. (n=3).

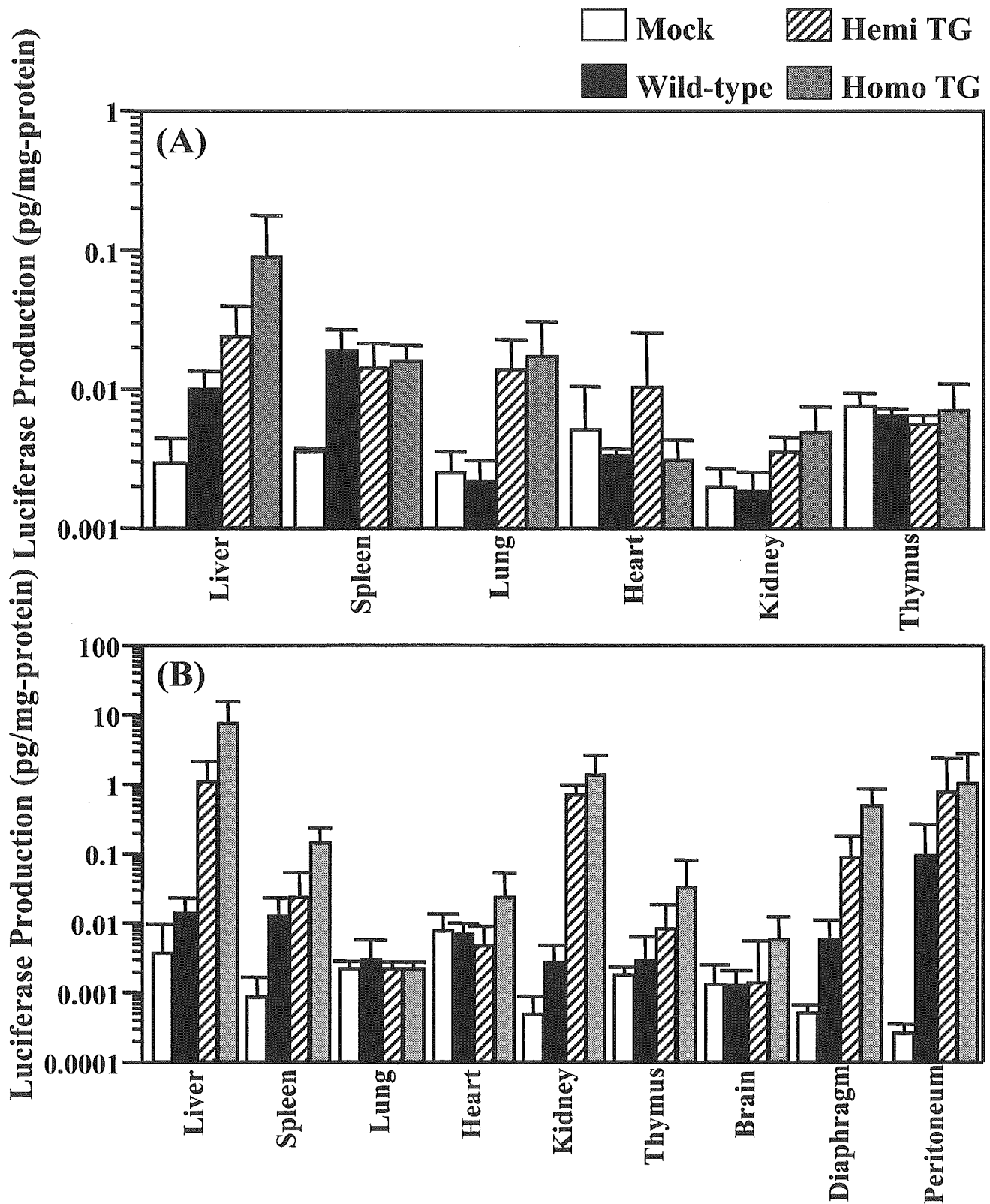


Fig. 83 Luciferase production in CD46TG and wild-type mice after intravenous and intraperitoneal administration of Ad35 vectors.

(A) Luciferase production after intravenous administration of the vector.

(B) Luciferase production after intraperitoneal administration. Ad35 vectors were administered to wild-type mice and hemizygous and homozygous CD46TG mice. After 48 h, the organs were harvested, and luciferase production was measured.

All data are represented as mean \pm S.D. (n = 4, intravenous administration; n = 6, intraperitoneal administration).

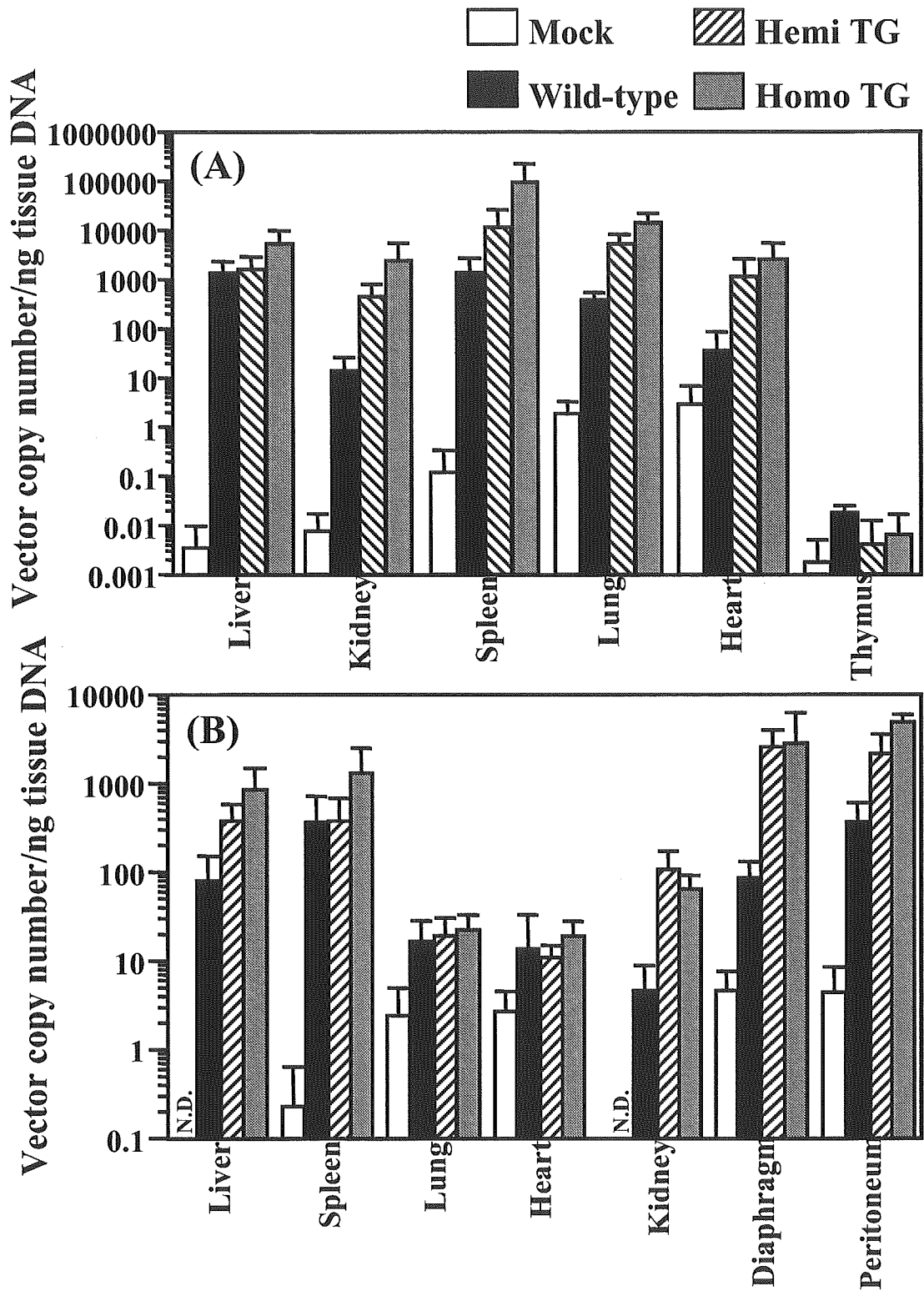


Fig. 84 Tissue distribution of viral DNA in CD46TG and wild-type mice after intravenous and intraperitoneal administration of Ad35 vectors.

(A) Ad35 vector DNA detected in organs after intravenous administration. (B) Ad35 vector DNA detected in organs after intraperitoneal administration. Ad35 vectors were administered to wild-type mice and hemizygous and homozygous CD46TG mice. After 48 h, the organs were harvested, and total DNA including viral DNA was extracted from the tissues after proteinase K digestion, and 25-ng samples of total DNA were subjected to quantitative real-time PCR. The data are represented as mean \pm S.D. (n = 4).

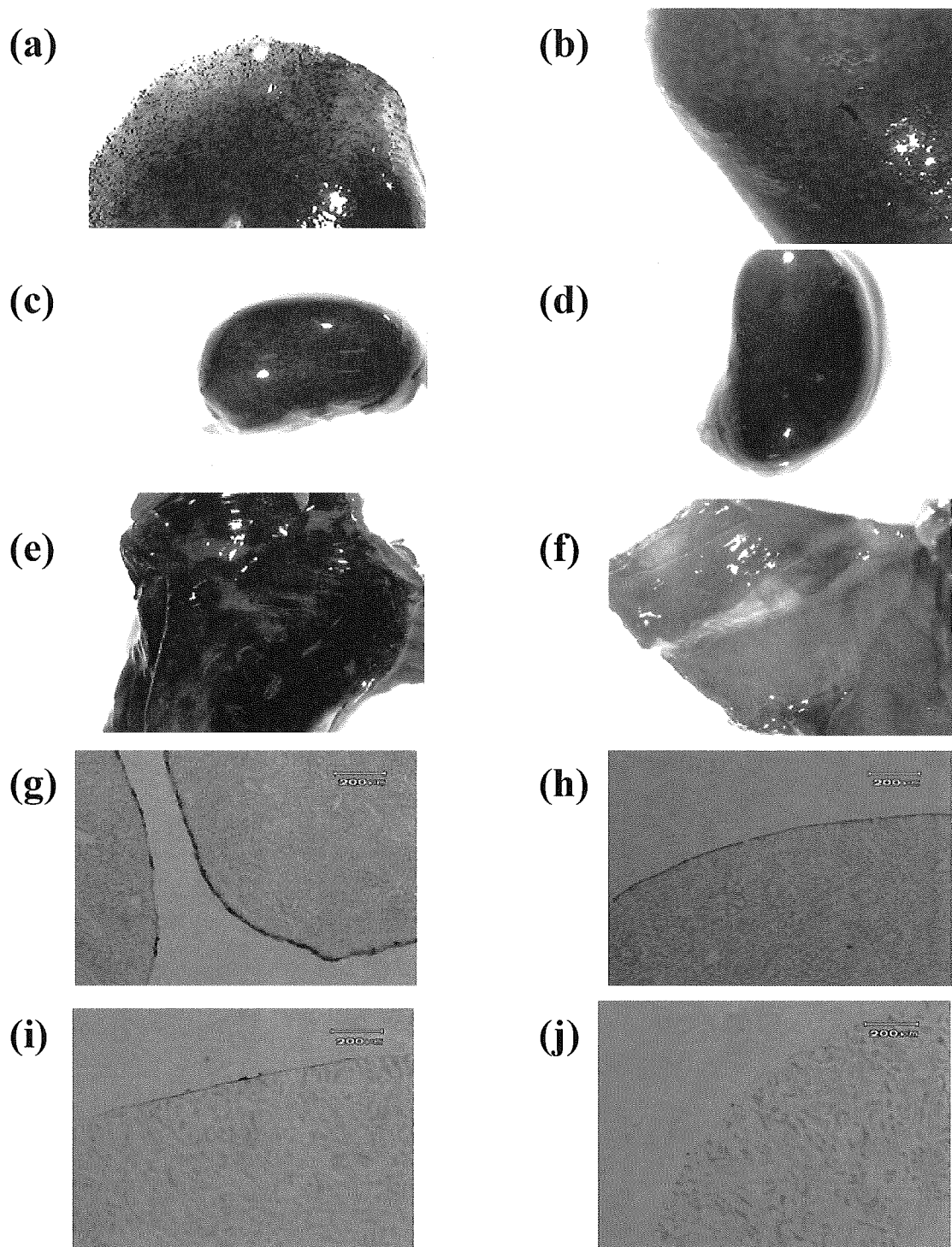


Fig. 85 X-gal staining of the peritoneal organs of homozygous CD46TG mice receiving β -galactosidase-expressing Ad35 vectors.

(a) Liver, (c) kidney, (e) peritoneum, (g) liver, and kidney sections from homo TG mice injected with Ad35 vectors. (b) Liver, (d) kidney, (f) peritoneum, (h) liver, and (j) kidney sections from mock-infected homo TG mice. Ad35 vectors were injected intraperitoneally into homozygous CD46TG mice. At 2 days postadministration, the organs were recovered after perfusion with 0.5% glutaraldehyde solution and then fixed and stained. For X-gal staining of liver and kidney, 10-mm sections were cut, fixed with 0.5% glutaraldehyde, and stained.

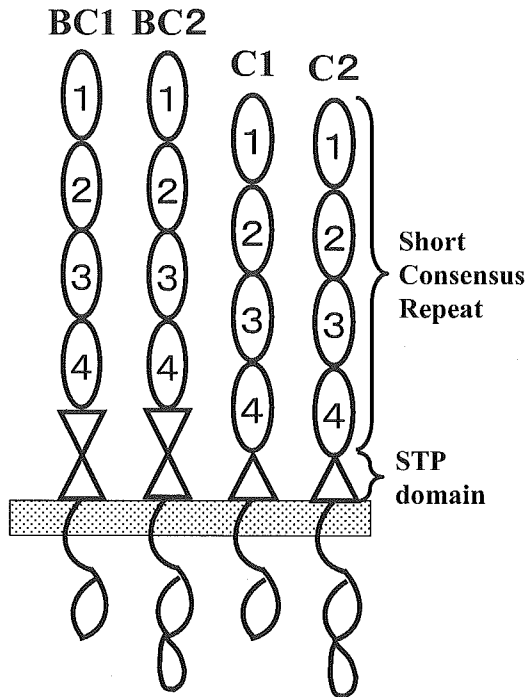


Fig.86 Structure of human CD46.

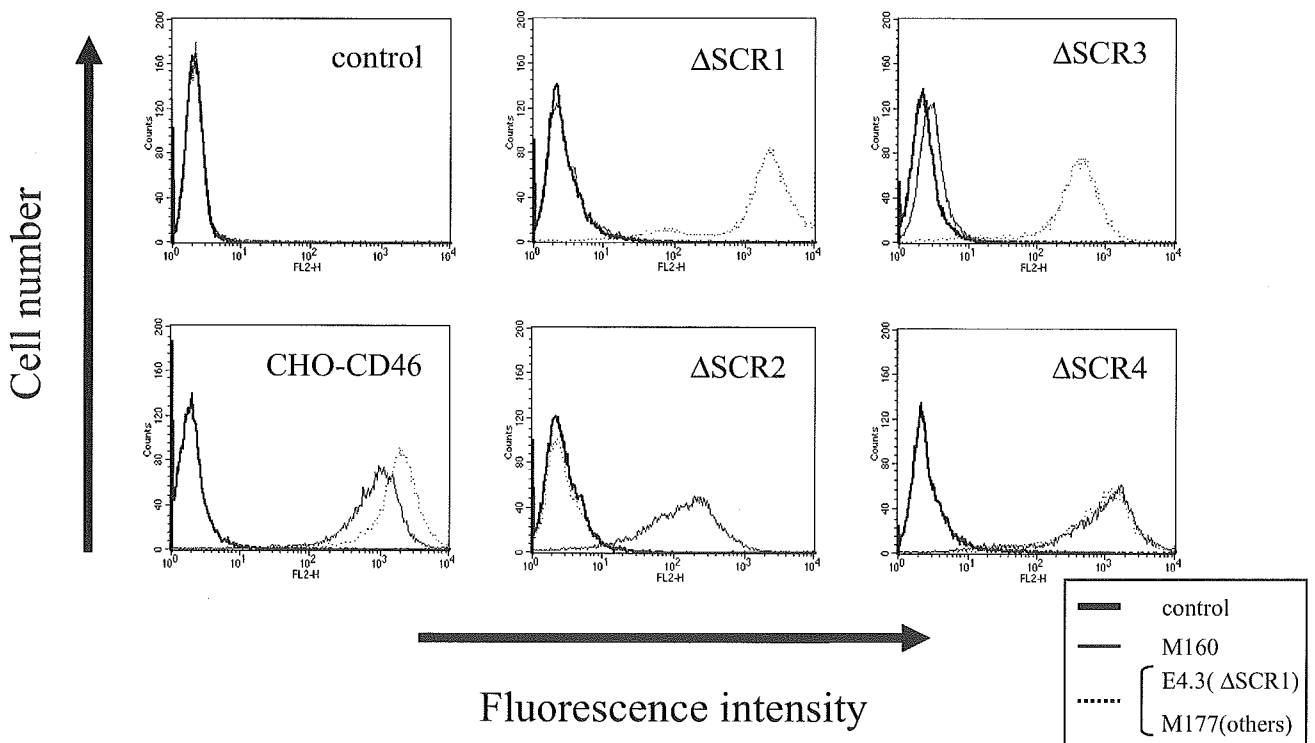


Fig.87 Expression profiles of CD46 deletion mutants detected by monoclonal anti-CD46 antibodies.

The cells were stained with anti-CD46 antibodies against SCR1 (E4.3), SCR2 (M177), or SCR3 (M160), and subsequently analyzed by flowcytometer.

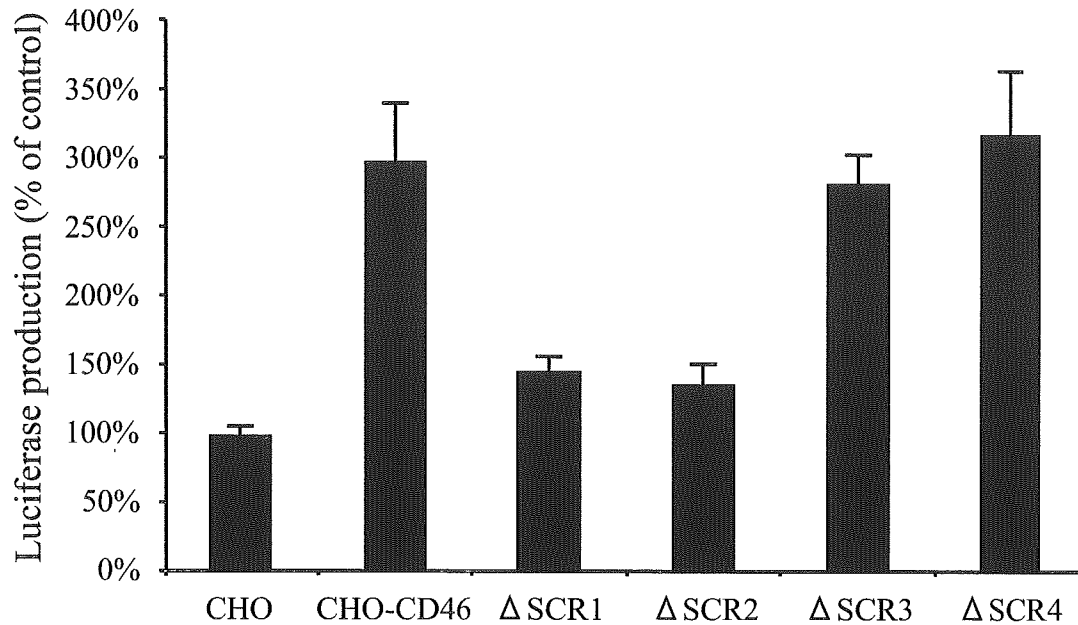


Fig.88 Ad35 vector-mediated transduction in CHO cells expressing CD46 mutants lacking SCRs. The cells were transduced with Ad35 vectors at 3000 VP /cells for 1.5 hr. The luciferase productions in the cells were measured 48 hr after transduction by luminescent assay. The data are expressed as mean \pm S.D. (n=4).

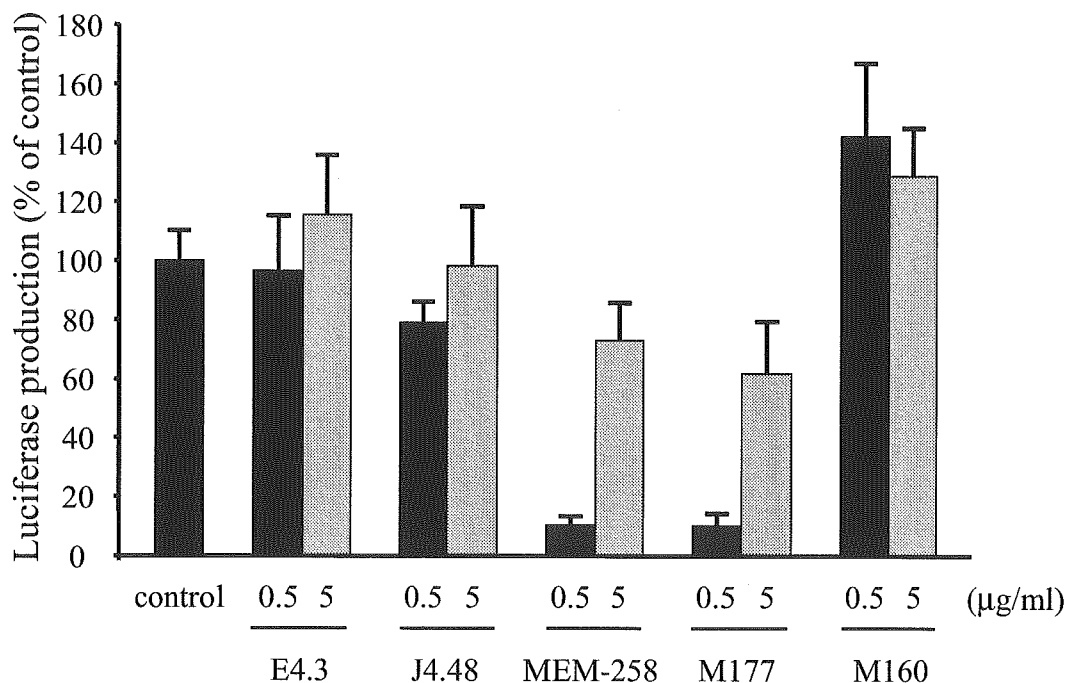


Fig.89 Blocking of Ad35 vector transduction by monoclonal anti-CD46 antibodies. E4.3, MEM-258, and J4-48 (recognizing SCR1), M177 (recognizing SCR2), and M160 (recognizing SCR3) were used as monoclonal anti-CD46 antibodies. CHO cells expressing wild-type CD46 were preincubated with each antibody at the indicated concentrations for 1 hr and then infected with Ad35 vectors expressing luciferase at 3000 VP/cell. The luciferase productions in the cells were measured by luminescent assay 48 hrs after transduction. In control settings (Control), the cells were preincubated with medium only prior to transduction. The data are expressed as mean \pm S.D. (n=4).

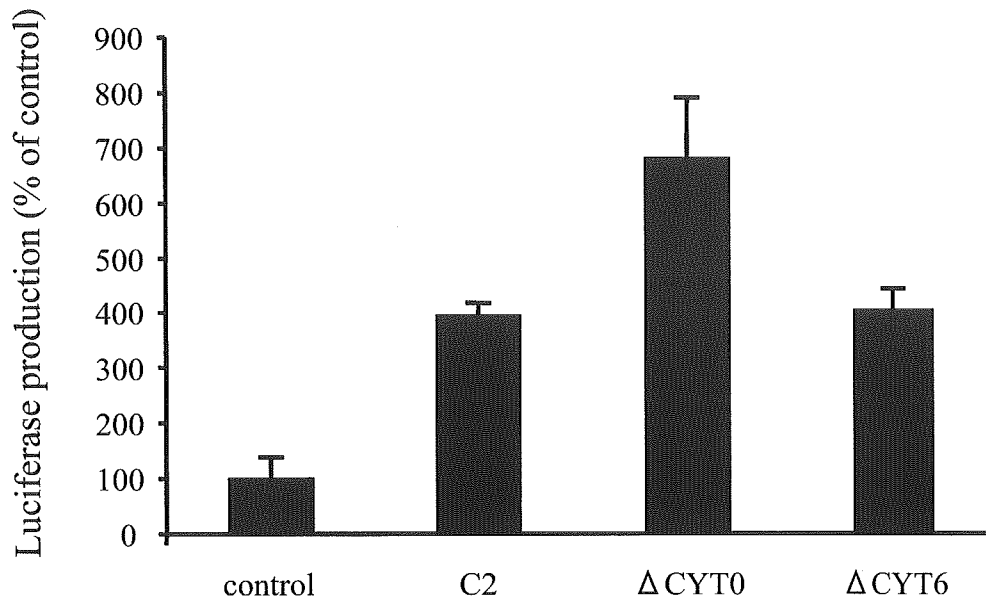


Fig.90 Ad35 vector-mediated transduction in CHO cells expressing CD46 mutants lacking the cytoplasmic domain. The cells, which were seeded the day before transfection, were transfected with plasmid encoding full-length CD46 or mutant CD46 lacking the cytoplasmic domain (CD46 Δ CYT0 and CD46 Δ CYT6). Twenty-four hr after transfection, the cells were transduced with Ad35 vectors at 3000 VP /cells for 1.5 hr. The luciferase productions in the cells were measured 48 hr after transduction by luminescent assay. The data are expressed as mean \pm S.D. (n=4).

次世代アデノウイルスベクターの開発基盤研究

分担研究者 中川晋作 大阪大学大学院薬学研究科 教授

本研究は、安全性が高く、機能面で優れたわが国独自の次世代遺伝子治療用ベクターの開発、および関連する遺伝子導入・発現技術に関する基盤研究を行うことを目的とする。その中で本年度は、サイトカインやケモカインを発現する RGD ファイバー改変型アデノウイルス (AdRGD) ベクターを用いたがん遺伝子治療応用研究、抗アポトーシス分子を発現する AdRGD ベクターを用いた樹状細胞 (DC) 療法応用研究、水溶性高分子 (PEG) によるバイオコンジュゲート化アデノウイルス (PEG-Ad) ベクターの特性解析とがん遺伝子治療応用研究、ならびに細胞膜透過ペプチド (Tat) を結合させたアデノウイルス (Tat-Ad) ベクターの作製とその遺伝子導入特性解析を行い、以下の結果を得た。

1. サイトカインとケモカインを発現する AdRGD ベクターを用いたがん免疫遺伝子治療の最適化を図った。その結果、マウスメラノーマに対する DC 免疫療法にケモカイン (CCL17) 発現 AdRGD ベクターの腫瘍内投与を併用することで、有効性を著しく改善することができた。また、IL-12 非奏功性腫瘍に IL-12 発現 AdRGD ベクターとケモカイン (CCL27) 発現 AdRGD ベクターを腫瘍内併用投与することで、抗腫瘍エフェクター細胞の腫瘍組織内動員とその活性化を同時に達成できることを明らかとし、強い抗腫瘍作用を得ることに成功した。
2. 抗アポトーシス分子を発現する AdRGD ベクターを用いた新規 DC 免疫療法を確立し、その有効性および作用機序を解析した。その結果、抗アポトーシス分子 (Bcl-x_L あるいは Bcl-xFNK) を発現する AdRGD ベクターで遺伝子導入した DC は、アポトーシス抵抗性を獲得し、投与部位から所属リンパ組織へと遊走する DC 数の増加と、そこでの DC 生存期間の延長に基づいて、抗腫瘍効果の誘導効率を大幅に改善できるワクチン担体であることを明らかとした。
3. PEG-Ad ベクターを用いたがん遺伝子治療の最適化を図った。その結果、治療用遺伝子 (TNF- α あるいは HSVtk) を搭載した PEG-Ad ベクターを用いることで、全身投与において未修飾 Ad ベクターよりも優れた腫瘍組織集積性 (EPR 効果) に基づく強力な抗腫瘍効果の誘導に成功した。さらに、PEG-Ad ベクターの遺伝子発現特性や体内動態に対する標的化リガンド (RGD ペプチド) の PEG 末端への導入あるいは修飾に用いる PEG の分子量の影響を明らかとした。
4. Tat-Ad ベクターの作製法を確立し、その遺伝子導入特性を解析した。その結果、Tat-Ad ベクターを用いることで、Ad 感染受容体の発現が乏しい細胞あるいは従来の Ad ベクターでは遺伝子導入効率が著しく低かった細胞に対して、非常に効率よく遺伝子導入することに成功した。

研究協力者

| | | | |
|------|----------------------------|------|----------------------------|
| 岡田直貴 | 大阪大学大学院薬学研究科 講師 | 衛藤佑介 | 大阪大学大学院薬学研究科 博士後期課程 1 年 |
| 吉川友章 | 大阪大学大学院薬学研究科 博士後期課程 3 年 | 櫻井晴奈 | 大阪大学大学院薬学研究科 博士後期課程 1 年 |

| | |
|-------|---------------------------|
| 金川尚子 | 大阪大学大学院薬学研究科 博士前期課程 2年 |
| 倉知慎之輔 | 大阪大学大学院薬学研究科 博士前期課程 2年 |
| 丹羽貴子 | 大阪大学大学院薬学研究科 博士前期課程 2年 |
| 森重智弘 | 大阪大学大学院薬学研究科 博士前期課程 1年 |
| 姚 醒蕾 | 大阪大学大学院薬学研究科 博士前期課程 1年 |
| 渡邊 光 | 大阪大学薬学部 4年生 |

A. 研究目的

アデノウイルス(Ad)ベクターは、標的細胞の分裂期・非分裂期を問わず極めて高い遺伝子導入効率を発揮することから、生命科学研究における遺伝子導入ツールとしてばかりでなく、遺伝子治療臨床研究においてもレトロウイルスベクターと並んで多用されている。また、作製法が簡便であり、遠心濃縮によって高力価のベクターが得られるなど、Adベクターは遺伝子治療用ベクターとして有利な基本特性を備えている。しかし一方で、Adベクターは生体内の種々の細胞に広く発現する coxsackie-adenovirus receptor (CAR) を標的とするため、その遺伝子導入を特定の組織や細胞に限定(ターゲティング)することは困難である。また、遺伝子治療の重要な標的細胞となるがん細胞や血球系細胞では、CARの発現が無いあるいは非常に乏しいために、Adベクター介在性遺伝子導入に対して抵抗性を示し、十分な治療効果を得るために高用量のベクターを適用すると、細胞・組織傷害性やAdベクターに対する過剰な免疫反応などの副作用発現に繋がる。したがって、有効性と安全性を兼ね備えたAdベクターによる遺伝子治療を実現するには、これらの問題点を克服しうる革新的アプローチを導入した改良型Adベクターを設計・創製し、それらの遺伝子導入特性と治療効果・副作用発現との関連評価を通して、最適な遺伝子治療用Adベクターシステムの確立に向けての基礎情報を収集することが不可欠である。

本観点から我々はこれまでに、遺伝子工学的にAdベクターのファイバー領域にRGDペプチドを表現させたRGDファイバー改変型Ad(AdRGD)ベクターが、標的指向性の拡大(α_v インテグリン指向性の付与)に基づいてCAR低発現細胞にも優れた遺伝子導入・発現効率を発揮することを見出し、このAdRGDベクターを用いてがん免疫遺伝子治療の最適化に繋がる方法論の構築に取り組んできた。また、Adベクター介在性遺伝子導入の組織標的化を達成する方法論として、水溶性高分子であるポリエチレングリコール(PEG)を用いてバイオコンジュゲート化したAd(PEG-Ad)ベクターの開発を行ってきた。

本年度は、遺伝子治療の最適化を目指したAdRGDベクターの応用研究として、免疫細胞の腫瘍組織集積性を増強しうる新規がん免疫遺伝子治療戦略、および樹状細胞(DC)ワクチンの利用能を向上しうる新規DCがん免疫療法戦略を提案し、それらの有効性ならびに作用メカニズムを精査した。また、PEG-Adベクターのがん遺伝子治療における有用性評価として、治療用遺伝子を搭載して全身投与した際の抗腫瘍効果を検討するとともに、PEG-Adベクターの遺伝子発現特性や体内動態の最適化(腫瘍標的化)に繋がる基礎情報の収集を図った。さらに、Adベクターの標的指向性のさらなる拡大を図るため、細胞膜透過ペプチドとして知られるTatペプチドによりベクター表面のカプシドタンパクを修飾したAd(Tat-Ad)ベクターの調製法を確立し、その遺伝子発現特性を解析した。

B. 研究方法

B.1. ベクターの作製、精製、および力価測定

従来型AdベクターおよびAdRGDベクターの作製は、水口らが開発したimproved *in vitro* ligation法に準拠した。

本研究に使用したベクターは、ホタルルシフェラーゼを発現するAd-LucおよびAdRGD-Luc、緑色蛍光タンパク(EGFP)を発現するAd-EGFP、ニワトリ卵白アルブミン(OVA)を発現するAdRGD-OVA、メラノーマ関連抗原の一つであるgp100を発現する